



HAL
open science

One-step versatile room temperature synthesis of metal(IV) carboxylate MOFs

Shan Dai, Farid Nouar, Sanjun Zhang, Antoine Tissot, Christian Serre

► **To cite this version:**

Shan Dai, Farid Nouar, Sanjun Zhang, Antoine Tissot, Christian Serre. One-step versatile room temperature synthesis of metal(IV) carboxylate MOFs. *Angewandte Chemie International Edition*, In press, 10.1002/anie.202014184 . hal-03052639

HAL Id: hal-03052639

<https://hal.science/hal-03052639>

Submitted on 23 Dec 2020

HAL is a multi-disciplinary open access archive for the deposit and dissemination of scientific research documents, whether they are published or not. The documents may come from teaching and research institutions in France or abroad, or from public or private research centers.

L'archive ouverte pluridisciplinaire **HAL**, est destinée au dépôt et à la diffusion de documents scientifiques de niveau recherche, publiés ou non, émanant des établissements d'enseignement et de recherche français ou étrangers, des laboratoires publics ou privés.

One-step versatile room temperature synthesis of metal(IV) carboxylate MOFs

Shan Dai^[a,b], Farid Nouar^[a], Sanjun Zhang^[b], Antoine Tissot^{*[a]}, Christian Serre^{*[a]}

[a] S. Dai, Dr. F. Nouar, Dr. A. Tissot, Dr. C. Serre
Institut des Matériaux Poreux de Paris, UMR 8004 Ecole Normale Supérieure, ESPCI Paris, CNRS, PSL University, 75005, Paris, France
E-mail: antoine.tissot@ens.psl.eu / christian.serre@ens.psl.eu

[b] S. Dai, S.J. Zhang
State Key Laboratory of Precision Spectroscopy, East China Normal University, No. 3663, North Zhongshan Road, Shanghai 200062, China

Supporting information for this article is given via a link at the end of the document.

Abstract: The development of room temperature green syntheses of robust MOFs is of great interest to meet the demand of the sustainable chemistry and is a pre-requisite for the incorporation of functional but fragile compounds in water stable MOFs. However, only few ambient conditions routes to produce metal(IV) based MOFs have been reported and most of them suffer from a very low yield and/or multiple steps that preclude their use for most applications. We report here a new versatile one-step synthesis of a series of highly porous M_6 oxoclusters based MOFs ($M = \text{Zr, Hf, Ce}$) at room temperature, including 8 or 12-connected micro/mesoporous solids with different functionalized organic ligands. The resulting compounds show varying degrees of defectivity, particularly for 12-connected phases, while maintaining the chemical stability of the parent MOFs. We propose first insights for the efficient MOF preparation based on *In-situ* kinetics observations. Remarkably, the synthetic versatility not only allows an efficient room temperature synthesis with a high space-time yield, but also gives possibility to tune the particle size, which therefore paves the way for their practical use.

Introduction

Room temperature (RT) green-synthesis of Metal-organic frameworks (MOFs) have generated interest in last two decades.^[1] In addition to the interest of industry for lower energy cost and safer conditions, the ambient conditions synthesis could also lead to some property enhancements (e.g. catalysis, gas adsorption) including the use of fragile compounds.^[2] Most low temperature routes reported to date deal with divalent metals based carboxylate MOFs. However, these solids strongly suffer from their poor chemical stability, particularly upon exposure to moisture, which prevents their practical use.^[3] With the more chemically robust Zeolitic Imidazolate Frameworks (ZIFs), low temperature synthesis allows however to construct core-shell materials through the direct formation of ZIFs in the presence of pre-formed functional molecules or nanoparticles in a view of several potential applications (sensing, catalysis, biomedicine...)^[4] Additionally, it is a convenient method to introduce low temperature-induced defects (LTID), as illustrated recently with the RT synthesis of ZIF-67 that led to the improvement of the catalytic activity for the synthesis of cyclic carbonates. It also allows using techniques that requires ambient conditions, such as the investigation of the MOF nucleation-growth kinetics at RT using in-situ Transmission-Electron-Microscope coupled with a liquid cell.^[5]

Trivalent metals (e.g. Fe, Al, Cr) based carboxylate MOFs are generally more chemically robust than the aforementioned divalent ones, particularly with Al(III) and Cr(III).^[6] In such case, the chemistry in play is more complex and developing versatile and easy room temperature synthesis routes is an old but still highly challenging objective.^[7] For example, despite efforts devoted to the sustainable synthesis of Trivalent-MOFs from the MIL family (MIL stands for Materials from Institut Lavoisier), only few of them can be so far synthesized using green solvents at room temperature, including MIL-53(Al), MIL-88A(Fe) and MIL-100(Fe).^[8]

Zr(IV) carboxylate based MOFs are considered as one of the most promising sub-class of MOFs due to their low toxicity and high chemical stability, making them appealing candidates for applications such as heterogeneous catalysis, gas/liquid

separation and bio-applications.^[9] These MOFs are typically synthesized using solvothermal conditions with toxic solvents such as DMF. Alternatively, one can synthesize these solids at ambient pressure using conventional^[10] or microwave-assisted heating.^[11]

In 2010, some of us reported a room temperature synthesis of UiO-66 type MOFs, starting from preformed Zr_6 oxoclusters and dicarboxylic acids in DMF.^[12] Since this pioneer study, the reaction of preformed Zr_6 / Zr_{12} oxoclusters with carboxylic acid linkers at room temperature using both solvent and solvent-free reactions has been explored.^[13] However, this strategy relies on the preparation of non-commercially available oxoclusters and in some cases gives rise to poorly crystalline solids with a relatively low yield. Despite the complexity of this RT method, it has been used to incorporate thermally sensitive compounds into Zr-MOFs. For example, Farha et al. reported the RT preparation of the 8-connected Zr-MOF NU-901 via a two steps approach, allowing the formation of core-shell Pd Nanorods@NU-901 for selective surface-enhanced Raman spectroscopy.^[14] RT routes to prepare metal(IV) MOFs is also of interest to produce LTID and tune their properties, including porosity, Lewis acidity and hydrophilicity.^[15]

Few recent reports describe one-step RT synthetic approaches of UiO-type MOFs.^[8b, 16] However, they rely on specific reactants or additives to promote nucleation, associated to cost issues and/or to the presence of impurities in the resulting products. Therefore, despite promises, there is still a strong need to develop a versatile simple higher yield and environmentally friendly RT approach to produce robust metal(IV) MOFs.

Here, we report a new more efficient one-step environmentally friendly route for the synthesis of metal(IV)-based MOFs at room temperature, including archetypical MOFs based either on 12-connected (MOF-801, UiO-66-NH₂, UiO-66-COOH) and 8-connected (DUT-67, PCN-222) M_6 oxoclusters ($M = \text{Zr, Hf, Ce}$). MOF-801 is used as a representative example in order to demonstrate the broad scope of available synthetic conditions, including the use of organic or inorganic Zr(IV) salts, of several tetravalent metal ions (Zr(IV), Hf(IV) or Ce(IV)) and of different types of modulators. In a second step, the extension of this strategy to several other benchmark MOFs is described. *In-situ* PXRD technique is finally considered to shed light on the nucleation/growth process, revealing the importance of the concentration on the synthetic efficiency. Finally, we demonstrate how our findings enable the successful laboratory pilot scale production of MOF-801, with a space-time yield (STY) of 168 kg/m³/day, among the highest for the RT synthesis of Zr-MOFs. We believe such novel green ambient conditions synthesis routes of Zr(IV)-carboxylate based MOFs could not only be extended to series of benchmark MOFs on a larger scale, paving the way towards their industrial production, but also be applied to combine MOFs with temperature sensitive species to develop new functional MOFs based composites.

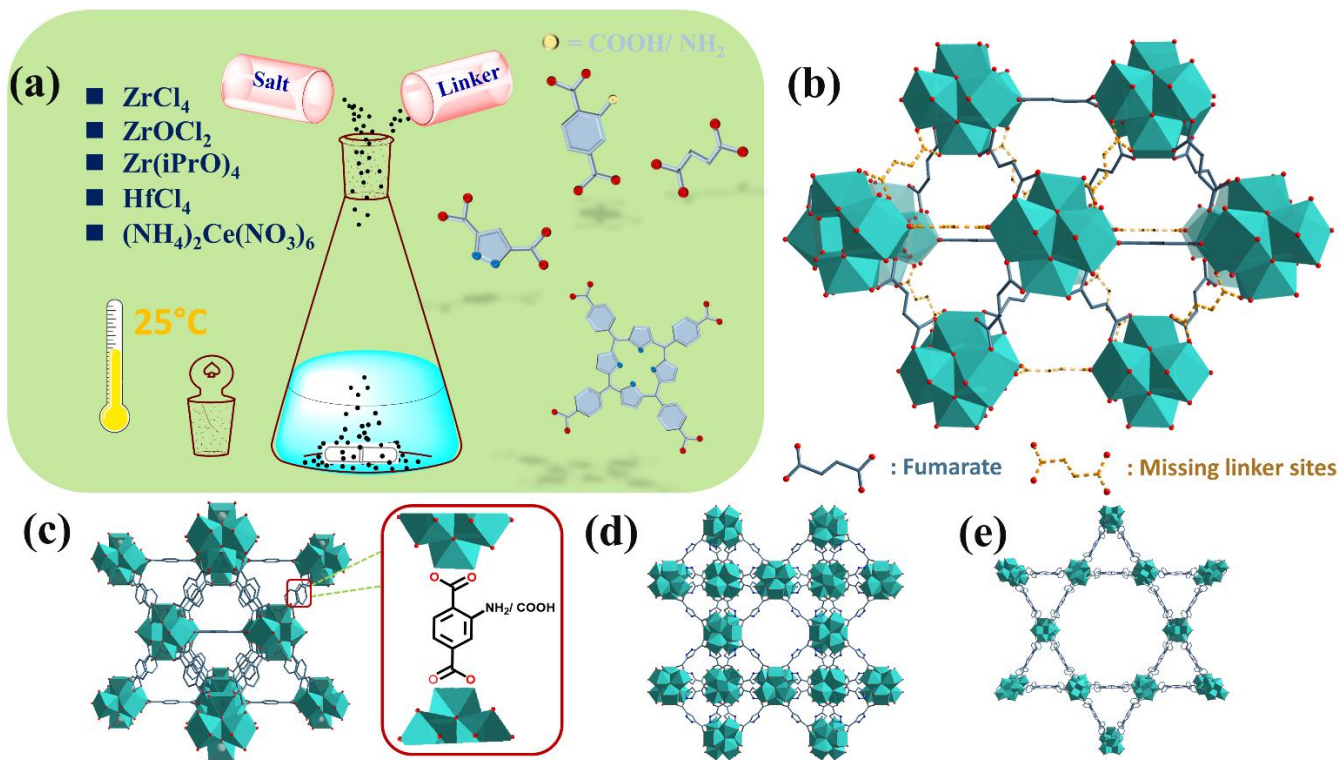


Figure 1. Schematic diagram of the room temperature one-step approach (a). Representative of the crystal structures of MOF-801(Zr, Hf, Ce) viewed along (101) plane and the illustration of existing defects (b), UiO-66-COOH/ NH₂ (c), DUT-67(PDA) (d) and PCN-222 (e). Metal polyhedra, carbon and oxygen atoms are in cyan, black and red, respectively (hydrogen atoms have been omitted for the sake of clarity).

Results and Discussion

MOF-801 or Zr-fumarate was selected as a prototypical example for our investigation due to the good solubility of fumaric acid in H₂O and the low price of the reactants. It presents a similar structure as UiO-66 with fumaric acid as linker instead of terephthalic acid. As illustrated in Figure 1(b), each Zr₆ oxocluster is coordinated to 12 fumaric acids, giving rise to a cubic 3D structure with two 5.6Å and 4.8Å types of tetrahedral

cages and one 7.4Å type of octahedral cage. PXRD patterns evidenced the successful synthesis of well-crystallized MOF-801 with Zr(IV), Hf(IV) and Ce(IV) in water at room temperature using formic acid as modulator (Figure 2(a)). Hf(IV)-based and Ce(IV)-based MOF analogues are usually less investigated comparing to Zr(IV) ones, despite their unique advantages in terms of high acidity and/or redox properties.^[17] A slight shift of the diffraction peaks was observed for MOF-801(Ce) due to the larger atomic radius of Ce(IV) compared to Zr(IV). Additionally, as formic acid is usually considered as a less favorable inhibitor due to its

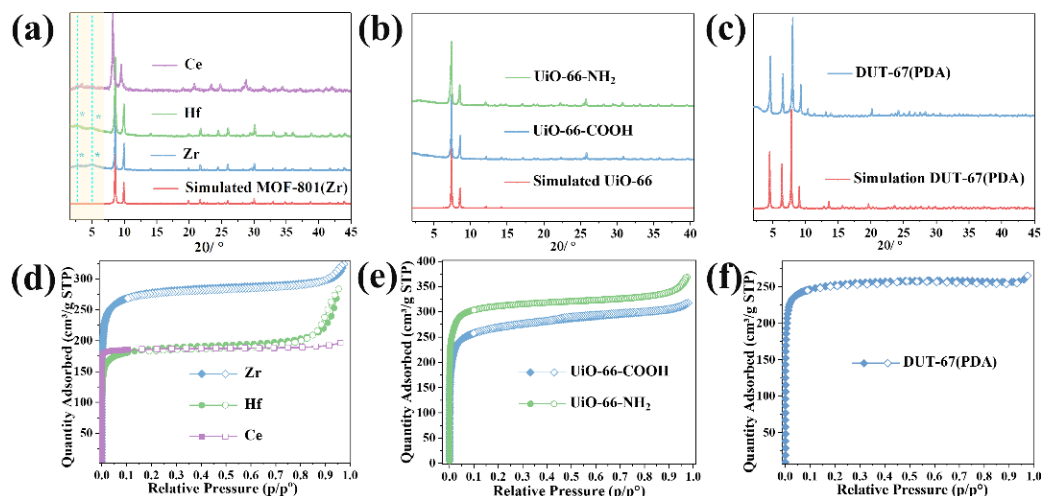


Figure 2. PXRD patterns ($\lambda_{\text{Cu}}=1.5406\text{\AA}$) of: (a) MOF-801(Zr), MOF-801(Hf), MOF-801(Ce), (b) UiO-66-NH₂ and UiO-66-COOH, (c) DUT-67(PDA) and the corresponding simulated PXRD patterns. N₂ adsorption-desorption isotherms (adsorption, filled symbols; desorption, empty symbols) at 77K ($P_0=1\text{ atm}$) of: (d) MOF-801(Zr), MOF-801(Hf), MOF-801(Ce), (e) UiO-66-NH₂ and UiO-66-COOH, (f) DUT-67(PDA).

higher acidic character, we also demonstrated the possibility (see Figure S15) to synthesize MOF-801(Zr) using acetic acid as inhibitor. The successful use of diverse metal salts in this approach, such as ZrOCl_2 and $\text{Zr}(\text{iPrO})_4$ for the synthesis of MOF-801(Zr) was also demonstrated (Figure S16). This is of interest particularly if one wants to minimize any corrosion or moisture stability issues when using ZrCl_4 . N₂ adsorption-desorption isotherms at 77K (Figure 2(d) and Table 1) evidenced that these materials are highly porous, with Brunauer-Emmett-

Teller (BET) surface area of $1035(\pm 5)$ m²/g (MOF-801(Zr)), $735(\pm 6)$ m²/g (MOF-801(Hf)) and $780(\pm 5)$ m²/g (MOF-801(Ce)) respectively. These values are slightly larger than the pristine MOF-801(Zr) (680 m²/g), which suggests that these MOFs present a significant amount of defects, as reported previously using other synthesis conditions.^[18] In order to determine the defect nature (missing nodes or linkers), FT-IR analysis was carried out (Figure S1). All the materials showed only vibrations associated to COO⁻ groups coordinated to Zr(IV), without traces of uncoordinated fumaric acid, suggesting that missing linkers are more plausible than missing nodes. Thermogravimetric analysis (TGA) further provided the evidence of the lower connectivity of the Zr₆ nodes compared to the ideal structure. According to the ratio of decomposed content of ligands and remaining metal oxide calculated from TGA (Table 1, Figure S2(a-c)), a connectivity between 7 and 10 is obtained depending on the samples, while a connectivity of 12 is expected for the perfect structure. Finally, in the case of MOF-801(Zr) and MOF-801(Hf), two low-intensity peaks at low angle (marked with blue dash line) appeared, in agreement with the presence of missing-linker defects in the body-centered initial *fcu* structure.^[19]

In a second step, we extended our strategy to a broader scope of Zr(IV)-based MOFs with different organic ligands and topologies to highlight the versatility of the approach. As shown in Figure 2(b, c), PXRD patterns evidenced that highly crystalline UiO-66-NH₂, UiO-66-COOH (*fcu* topology, see structure in Figure 1(c)) and DUT-67(PDA) (*reo* topology, see structure in Figure 1(d)) were synthesized successfully following a similar synthesis protocol. Notably, synthesizing the functionalized UiO-66-COOH at room temperature is not straightforward due to the lower pKa of Trimellitic acid in comparison to other derivatives (e.g. -NH₂, -H) that usually favors the formation of amorphous compounds.^[8b, 13c] The room temperature obtained MOFs presented higher surface areas (UiO-66-NH₂ ($1255(\pm 5)$ m²/g), UiO-66-COOH ($1050(\pm 6)$ m²/g) and DUT-67(PDA) ($1020(\pm 6)$ m²/g)) than the theoretical values (see Figure 2(e, f)), in agreement with the presence of defects, as mentioned above for MOF-801 (see Table 1). Pore size distribution for UiO-type MOFs (see Figure S10(a, b)) revealed indeed the defect-engineering pore size expansion, showing a wide pore size distribution from 0.6 to 1.6 nm, which is much larger than the one deduced from the crystal structures^[20]. In the latter case, DUT-67(PDA) showed a similar 77K N₂ adsorption capacity than the reported one obtained on a compound prepared using solvothermal synthesis. This is in agreement with TGA, which indicates that only 0.2 linker per metal nodes are missing in this case.^[21]

In addition to the use of short dicarboxylic ligands described above, PCN-222, a highly chemically stable MOF based on a 4,8-connected framework (see structure in Figure 1(e)) comprising Zr₆ oxoclusters and TCPP (tetrakis(4-carboxyphenyl)porphyrin), was synthesized at room temperature.^[22] Due to the poor solubility of TCPP in many solvents, including DMF, we used Zr(iPrO)₄ (Zirconium(IV) isopropoxide), a more basic zirconium source than ZrCl₄ and ZrOCl₂ that may enhance the linker solubility via a partial deprotonation of TCPP. Figure 3(a) shows that highly crystalline PCN-222 microcrystals were obtained, confirming that our room temperature synthesis strategy is also suitable for metal(IV) carboxylate MOFs built with large poorly soluble ligands. Even

though the product yield (56%) is lower than for the other cases presented in this work, it is still comparable with the reported one using high-temperature synthesis in DMF.^[22] Apart from the low solubility of TCPP in EtOH, the contamination of the product during the synthesis by coordination of TCPP to unsaturated Zr sites in the large hexagonal pores of the MOF can further decrease the product yield. Notably, when one considers the preparation MOFs based on polyphenylene ligands and high valence metal ions, mixed phases are often obtained, which was not the case here as confirmed by PXRD and SEM (Figure S11).^[23] N₂ adsorption-desorption isotherms in Figure 3(b) showed high porosity and a typical shape of isotherm due to the hierarchical pore of PCN-222.

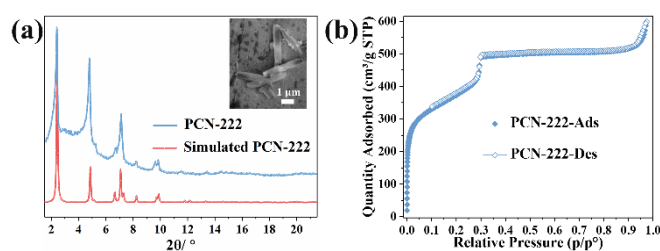


Figure 3. (a) Experimental and simulated PXRD patterns ($\lambda_{Cu}=1.5406\text{\AA}$) of PCN-222, (b) N₂ adsorption-desorption isotherm at 77K of PCN-222 (P0=1 atm).

In order to investigate the chemical stability of all these synthesized MOFs, the compounds were soaked in different chemical environments (initial pH= 0, 12, boiling water for 2 days). PXRD measurements in Figure S3-9 proved that all these materials present -as previously reported- a high chemical stability even in presence of a large amount of missing ligands.

The above-mentioned results demonstrated the versatility of this new environmentally friendly synthesis approach. We then investigated the possibility to take benefit from this strategy to produce nanosized MOFs (nanoMOFs). These latter have been extensively studied for their appealing advantages in catalysis, sensing, bio-applications and membrane science.^[24] Usually, the particle size tuning was realized following several strategies such as microwave heating, sonication, fluidics, or the use of emulsions, modulators, shorter reaction time or temperature control.^[25] In spite of diverse synthetic methods, a scalable green synthesis of nanoMOFs with high product yield is still highly demanded and only few examples have been reported so far.^[26] Here, in the case of MOF-801(Zr), decreasing the amount of modulator allowed particle size tuning from ~220 nm to ~45 nm according to SEM, TEM images (Figure S12 and Figure S13) and PXRD (see broadening of the Bragg peaks on Figure S14). Noteworthy, whatever the particle size, a well-crystalline MOF-801(Zr) without any decrease of the yield (89%).

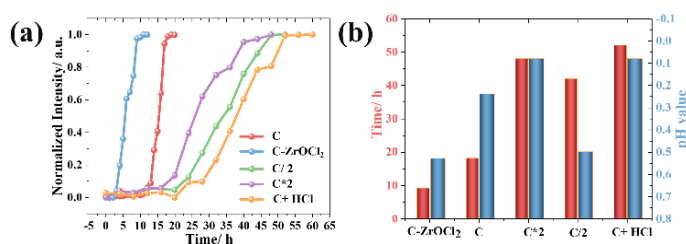


Figure 4. (a) Plot of synthesis time versus the intensities of the strongest (1, 1) reflection of MOF-801 with varying precursors concentrations (the reactions

were considered saturated when the intensities did not grow significantly), C represented the MOF-801 synthesized in 0.15 mmol/ mL precursors concentration, C*2 represented the 2 times multiple concentration, C/2 represented the 2 times divided concentration, C-ZrOCl₂ represented the MOF-801 synthesized with ZrOCl₂ in 0.15 mmol/ mL concentration, C+ HCl represented the MOF-801 synthesized in 0.15 mmol/ mL reactant with the presence 0.6 mmol/ L of HCl. (b) Correlations between the synthesis time and pH value for samples described in (a).

In order to prepare Zr-MOFs at ambient temperature without any detrimental effect on the kinetics of nucleation, the lowering of activation energies is needed. Previous reports showed that activation energies of nucleation and growth are close for UiO-type MOFs (71 kJ mol⁻¹ vs 66 kJ mol⁻¹).^[27] Few factors have been found to lower down these values, including the addition of HCl,^[28] water and/or the use of more soluble ligands.^[27, 29] In our case, the mixture of ZrCl₄ (or ZrOCl₂) and pure H₂O (~300 equiv H₂O/ Zr) led to relatively low pH values (≈0.24, experimentally) in comparison to the conventional synthesis in DMF but hydrolysis of Zr⁴⁺ species was favored by the excess of water that led to the easier formation of Zr₆ oxoclusters with bridging μ₃-O and μ₃-OH groups. Thus, this might explain why our conditions favor the formation of Zr₆ oxoclusters at room temperature.^[30] Moreover, the Arrhenius activation energies for the MOF growth were expected to be relatively low owing to the reasonable solubility of the chosen linkers in H₂O/ Ethanol. The temperature-dependent *in-situ* nucleation experiments reported previously in the presence of H₂O, ZrCl₄/ ZrOCl₂, HCl, and DMF by some of us indicated that lowering down the temperature had a significantly negative impact on the nucleation time of UiO-66, particularly when the temperature was lower than 90°C.^[28] In a nut-shell, the nucleation time was increased ca. 2 times when decreasing every 10°C. Accordingly, keeping identical the other synthesis parameters, the nucleation time should have reached almost 40 days at room temperature. In our case, the synthesis time was only of 1-2 days (spinning in a capillary). Thus, apart from the synthetic parameters aforementioned, we hypothesize that the use of lower concentrations of Zr precursors here probably compensate the lower temperature due to the less acidic pHs of the solutions. Indeed, higher pH most likely accelerate the nucleation/growth process as the ligands are more easily deprotonated and the formation of Zr oxo-clusters is favored in such conditions.^[28, 31] To verify such assumptions, we followed *in-situ* the nucleation-growth processes at room temperature using PXRD (shown in Figure S17-21) in order to estimate kinetics parameters. It can be concluded that 1) no intermediate states were detected during the synthesis process, 2) nucleation-growth processes of MOF-801 at different concentrations (0.3 mmol/mL and 0.075 mmol/mL) (Figure 4(a-b)) were twice longer (48h, 42h, respectively) than that of MOF-801 at 0.15 mmol/mL. This means that further tuning the concentration, higher or lower, is here not advantageous if one wants to faster the synthesis of MOF-801. When considering a higher concentration (0.3 mmol/mL), the solution becomes more acidic (initial pH=0.08), which may slightly inhibit the MOF growth and slow down its crystallization. To confirm this point, a synthesis was performed with the initial reactant concentrations (0.15 mmol/mL) in presence of 0.6 mmol/mL of HCl. The addition of HCl lowers the initial pH to a value similar to the synthesis performed with 0.3 mmol/mL reactant concentrations. The kinetics showed a similar trend in both cases, strongly

evidencing the detrimental effect of low initial pH on the reaction kinetics. When using a lower concentration (0.075 mmol/ mL, pH= 0.50), we hypothesize than even if the pH is slightly higher, the high dilution of the reactants may lead to a deceleration of the kinetics. Additionally, when replacing ZrCl₄ by the less acidic ZrOCl₂ while keeping other parameters unchanged, faster nucleation-growth processes (from 19 h to 9h) were observed as a consequence of the presence of pre-formed Zr-oxo or Zr-OH bonds in ZrOCl₂. As a whole, our findings reveal that in addition to the typical parameters investigated so far (temperature, pH, metal source...), the concentration of the reactants is also playing a key role in the synthesis of Zr-MOF, particularly at room temperature.

Room temperature synthesis of Metal (IV) based MOFs, with its lower energy penalty and safer conditions, endows a great potential for a more sustainable industrial production, particularly for more robust Zr-MOFs. However, the previous examples of lab-scale synthesis of MOFs at room temperature led in most cases to very low space-time yields (STY), less than 1 kg/m³/day,^[32] which does not meet at all the needs of industry. In the case of Zr-MOFs, this is mainly due to their prolonged synthesis time at room temperature.^[33] Taking benefit from our preliminary crystallization study, we therefore scaled-up the benchmark Zr MOF MOF-801 by using a 5L pilot scale reactor with mechanical stirring (Figure 5(a)).

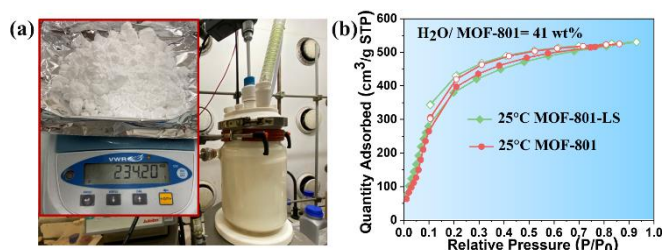


Figure 5. (a) 5L glass reactor laboratory pilot scale system for the upscaling synthesis of MOF-801-LS (large scale), inserted picture: mass of product after synthesis, washing and drying, (b) Water sorption isotherms (adsorption, filled symbols; desorption, open symbols) of MOF-801-LS (large-scale) and MOF-801 (lab-scale) at 25°C.

The space-time yield of the product was calculated according to the dry solid collected after washing and drying steps, reaching 168 kg/m³/day. To the best of our knowledge, this is the first example of room temperature synthesized Zr-MOF with such a high space-time yield. This quality of a scaled-up material in comparison with a small scale laboratory sample is also a prerequisite for industrial applications. As MOF-801 is a prominent example of sorbent suitable for heat reallocation applications,^[34] we investigated the water sorption properties (Figure 5(b)) of our scaled up material. Noteworthy it led to a consistently highly crystalline solid in comparison to the lab-scale synthesis (see Figure S22), attaining a remarkably high water adsorption capacity of 41 wt% H₂O/ MOF. The isotherm is of a Type-I shape mainly due to the presence of defects in the structure, which on the one hand increases the hydrophilicity due to the increased Coulomb interaction from the hydroxyl terminal group at the defect sites, while on the other hand expands the pore volume of the MOF due to the missing linker effect aforementioned.

Table 1. Summary of the properties of room temperature synthesized MOFs presented in this work

Entry	Materials	Connectivity	Solvent	BET Surface area (m ² /g)	Pore size (nm)	Pore volume (cm ³ /g)	Coordination number of each Zr _n /TNCL [#]
1	MOF-801(Zr)	12-connected	H ₂ O	1035	1.2	0.43	4.1/ 6
2	MOF-801(Hf)	12-connected	H ₂ O	737	0.8	0.26	3.5/ 6
3	MOF-801(Ce)	12-connected	H ₂ O	781	0.6	0.3	5.3/ 6
4	UiO-66-NH ₂	12-connected	H ₂ O EtOH	1256	0.7, 1.5	0.5	4.7/ 6
5	UiO-66-COOH	12-connected	H ₂ O	1052	0.8, 1.2	0.4	3.8/ 6
6	DUT-67(PDA)	8-connected	H ₂ O	1018	0.7, 1.2	0.41	3.8/ 4
7	PCN-222	8-connected	H ₂ O EtOH	1394	1.2, 1.6, 3.5	0.86	1.5/ 2

#TNCL[#] Theoretical number of coordinated ligands

Conclusion

In summary, we report here a new facile and versatile approach for the one-step synthesis of a series of highly porous metal(IV) carboxylate MOFs (M=Zr, Hf, Ce) including five 12-connected and two 8-connected MOFs, using greener ambient temperature conditions. Not only this allowed us to produce high quality crystalline and porous robust metal(IV) carboxylate MOFs with varying metal salts, but also, through a tuning of the synthetic parameters, enabled a control the MOF particle size at the nanoscale. Finally, we evaluated the possibility of scaling-up the synthesis with the use of 5L pilot scale system, evidencing a highest space-time yield for the room temperature synthesis of MOF-801(Zr). As a whole, our method paves the way for the versatile RT synthesis of series of metal(IV)-MOFs that is of strong interest for many applications as well as for their industrial production under sustainable conditions.

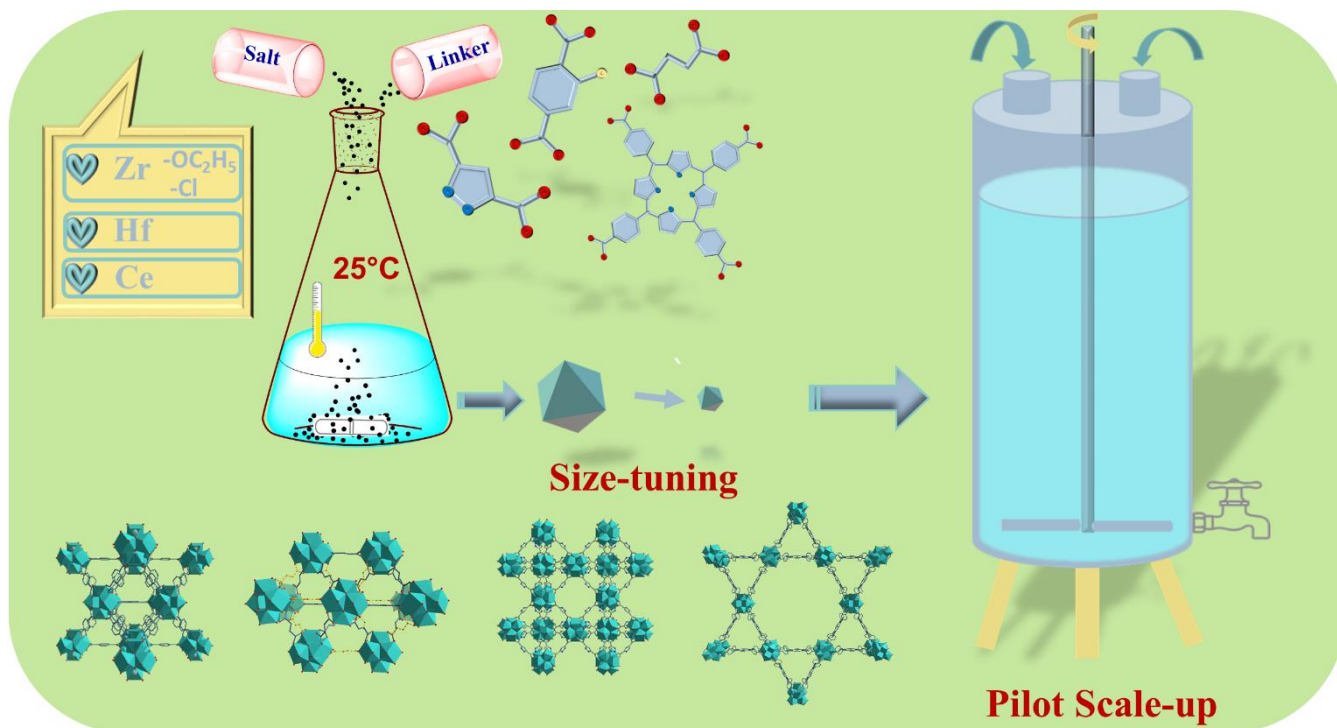
Acknowledgements

S. Dai acknowledges the support of CSC scholarship (201706140196).

Keywords: Metal (IV) Metal-organic frameworks •Room temperature synthesis • Defective MOF • Scale-up synthesis

- [1] S. Yuan, L. Feng, K. C. Wang, J. D. Pang, M. Bosch, C. Lollar, Y. J. Sun, J. S. Qin, X. Y. Yang, P. Zhang, Q. Wang, L. F. Zou, Y. M. Zhang, L. L. Zhang, Y. Fang, J. L. Li, H. C. Zhou, *Adv. Mater.* **2018**, *30*.
- [2] a) P. A. Julien, C. Mottillo, T. Friscic, *Green Chem.* **2017**, *19*, 2729-2747; b) Q. Gao, S. Y. Xu, C. Guo, Y. G. Chen, L. Y. Wang, *ACS Appl. Mater. & Interfaces.* **2018**, *10*, 16059-16065; c) D. S. Sholl, R. P. Lively, *J. Phys. Chem. Lett.* **2015**, *6*, 3437-3444.
- [3] A. J. Howarth, Y. Y. Liu, P. Li, Z. Y. Li, T. C. Wang, J. Hupp, O. K. Farha, *Nat. Rev. Mater.* **2016**, *1*, 15.
- [4] G. Lu, S. Li, Z. Guo, O. K. Farha, B. G. Hauser, X. Qi, Y. Wang, X. Wang, S. Han, X. Liu, J. S. DuChene, H. Zhang, Q. Zhang, X. Chen, J. Ma, S. C. Loo, W. D. Wei, Y. Yang, J. T. Hupp, F. Huo, *Nat. Chem.* **2012**, *4*, 310-316.
- [5] a) J. P. Patterson, P. Abellan, M. S. Denny, C. Park, N. D. Browning, S. M. Cohen, J. E. Evans, N. C. Gianneschi, *J. Am. Chem. Soc.* **2015**, *137*, 7322-7328; b) J. W. Hou, P. D. Sutrisna, Y. T. Zhang, V. Chen, *Angew. Chem., Int. Ed.* **2016**, *55*, 3947-3951; c) C. X. Duan, Y. Yu, P. F. Yang, X. L. Zhang, F. E. Li, L. B. Li, H. X. Xi, *Ind. Eng. Chem. Res.* **2020**, *59*, 774-782; d) B. Q. Yuan, X. Wang, X. Zhou, J. Xiao, Z. Li, *Chem. Eng. J.* **2019**, *355*, 679-686.
- [6] a) G. Ferey, C. Mellot-Draznieks, C. Serre, F. Millange, J. Dutour, S. Surble, I. Margiolaki, *Science* **2005**, *309*, 2040-2042; b) C. Serre, F. Millange, C. Thouvenot, M. Nogues, G. Marsolier, D. Louer, G. Ferey, *J. Am. Chem. Soc.* **2002**, *124*, 13519-13526.
- [7] S. J. Wang, C. Serre, *Accs Sustainable Chem. Eng.* **2019**, *7*, 11911-11927.
- [8] a) M. Sanchez-Sanchez, N. Getachew, K. Diaz, M. Diaz-Garcia, Y. Chebude, I. Diaz, *Green Chem.* **2015**, *17*, 1500-1509; b) C. Avci-Camur, J. Perez-Carvajal, I. Imaz, D. Maspoch, *Accs Sustainable Chem. Eng.* **2018**, *6*, 14554-14560; c) K. Guesh, C. A. D. Caiuby, A. Mayoral, M. Diaz-Garcia, I. Diaz, M. Sanchez-Sanchez, *Cryst. Growth & Des.* **2017**, *17*, 1806-1813; d) C. Serre, F. Millange, S. Surblé, G. Férey, *Angew. Chem.* **2004**, *116*, 6445-6449.
- [9] a) C. C. Cao, C. X. Chen, Z. W. Wei, Q. F. Qiu, N. X. Zhu, Y. Y. Xiong, J. J. Jiang, D. W. Wang, C. Y. Su, *J. Am. Chem. Soc.* **2019**, *141*, 2589-2593; b) G. D. Pirngruber, L. Hamon, S. Bourrelly, P. L. Llewellyn, E. Lenoir, V. Guillerm, C. Serre, T. Devic, *ChemSusChem* **2012**, *5*, 762-776; c) M. H. Teplerisky, M. Fantham, P. Li, T. C. Wang, J. P. Mehta, L. J. Young, P. Z. Moghadam, J. T. Hupp, O. K. Farha, C. F. Kaminski, D. Fairen-Jimenez, *J. Am. Chem. Soc.* **2017**, *139*, 7522-7532.
- [10] a) S. Rapti, A. Pournara, D. Sarma, I. T. Papadas, G. S. Armatas, Y. S. Hassan, M. H. Alkordi, M. G. Kanatzidis, M. J. Manos, *Inorg. Chem. Front.* **2016**, *3*, 635-644; b) Q. Y. Yang, S. Vaesen, F. Ragon, A. D. Wiersum, D. Wu, A. Lago, T. Devic, C. Martineau, F. Taulelle, P. L. Llewellyn, H. Jobic, C. L. Zhong, C. Serre, G. De Weireld, G. Maurin, *Angew. Chem., Int. Ed.* **2013**, *52*, 10316-10320.
- [11] H. Reinsch, S. Waitschat, S. M. Chavan, K. P. Lillerud, N. Stock, *Eur. J. Inorg. Chem.* **2016**, 4490-4498.
- [12] V. Guillerm, S. Gross, C. Serre, T. Devic, M. Bauer, G. Ferey, *Chem. Commun. (Camb)* **2010**, *46*, 767-769.
- [13] a) B. Karadeniz, A. J. Howarth, T. Stolar, T. Islamoglu, I. Dejanović, M. Tireli, M. C. Wasson, S.-Y. Moon, O. K. Farha, T. Friščić, K. Užarević, *Accs Sustainable Chem. Eng.* **2018**, *6*, 15841-15849; b) A. M. Fidelli, B. Karadeniz, A. J. Howarth, I. Huskic, L. S. Germann, I. Halasz, M. Etter, S. Y. Moon, R. E. Dinnebier, V. Stilianovic, O. K. Farha, T. Friscic, U. Z. K. *Chem. Commun. (Camb)* **2018**, *54*, 6999-7002; c) M. R. DeStefano, T. Islamoglu, J. T. Hupp, O. K. Farha, *Chem. Mater.* **2017**, *29*, 1357-1361.
- [14] a) H. Noh, C.-W. Kung, T. Islamoglu, A. W. Peters, Y. Liao, P. Li, S. J. Garibay, X. Zhang, M. R. DeStefano, J. T. Hupp, O. K. Farha, *Chem. Mater.* **2018**, *30*, 2193-2197; b) J. W. M. Osterrieth, D. Wright, H. Noh, C. W. Kung, D. Vulpe, A. Li, J. E. Park, R. P. Van Duyne, P. Z. Moghadam, J. J. Baumberg, O. K. Farha, D. Fairen-Jimenez, *J. Am. Chem. Soc.* **2019**, *141*, 3893-3900.
- [15] a) X. Feng, J. Hajek, H. S. Jena, G. B. Wang, S. K. P. Veerapandian, R. Morent, N. De Geyter, K. Leysens, A. E. J. Hoffman, V. Meynen, C. Marquez, D. E. De Vos, V. Van Speybroeck, K. Leus, P. Van Der Voort, *J. Am. Chem. Soc.* **2020**, *142*, 3174-3183; b) J. Choi, L.-C. Lin, J. C. Grossman, *J. Phys. Chem. C* **2018**, *122*, 5545-5552; c) C. A. Clark, K. N. Heck, C. D. Powell, M. S. Wong, *Accs Sustainable Chem. Eng.* **2019**, *7*, 6619-6628.
- [16] X. Sang, J. Zhang, J. Xiang, J. Cui, L. Zheng, J. Zhang, Z. Wu, Z. Li, G. Mo, Y. Xu, J. Song, C. Liu, X. Tan, T. Luo, B. Zhang, B. Han, *Nat. Commun.* **2017**, *8*, 175.
- [17] a) S. Rojas-Buzo, P. García-García, A. Corma, *Green Chem.* **2018**, *20*, 3081-3091; b) M. Lammert, M. T. Wharmby, S. Smolders, B. Bueken, A. Lieb, K. A. Lomachenko, D. De Vos, N. Stock, *Chem. Commun.* **2015**, *51*, 12578-12581.
- [18] J. Choi, L. C. Lin, J. C. Grossman, *J. Phys. Chem. C* **2018**, *122*, 5545-5552.
- [19] G. C. Shearer, S. Chavan, J. Ethiraj, J. G. Vitillo, S. Svelle, U. Olsbye, C. Lamberti, S. Bordiga, K. P. Lillerud, *Chem. Mater.* **2014**, *26*, 4068-4071.
- [20] a) J. H. Cavka, S. Jakobsen, U. Olsbye, N. Guillou, C. Lamberti, S. Bordiga, K. P. Lillerud, *J. Am. Chem. Soc.* **2008**, *130*, 13850-13851; b) G. R. Cai, H. L. Jiang, *Angew. Chem., Int. Ed.* **2017**, *56*, 563-567.
- [21] a) V. Bon, I. Senkovska, I. A. Baburin, S. Kaskel, *Cryst. Growth & Des.* **2013**, *13*, 1231-1237; b) J. Jacobsen, H. Reinsch, N. Stock, *Inorg. Chem.* **2018**, *57*, 12820-12826.
- [22] D. Feng, Z. Y. Gu, J. R. Li, H. L. Jiang, Z. Wei, H. C. Zhou, *Angew. Chem., Int. Ed.* **2012**, *51*, 10307-10310.
- [23] H. Q. Xu, K. Wang, M. Ding, D. Feng, H. L. Jiang, H. C. Zhou, *J. Am. Chem. Soc.* **2016**, *138*, 5316-5320.
- [24] a) M. Sindoro, N. Yanai, A. Y. Jee, S. Granick, *Accounts Chem. Res.* **2014**, *47*, 459-469; b) O. Shekhan, J. Liu, R. A. Fischer, C. Woll, *Chem. Soc. Rev.* **2011**, *40*, 1081-1106.
- [25] a) W. Morris, S. Z. Wang, D. Cho, E. Auyeung, P. Li, O. K. Farha, C. A. Mirkin, *ACS Appl. Mater. & Interfaces.* **2017**, *9*, 33413-33418; b) H. Bunzen, M. Grzyba, M. Hambach, S. Spirkl, D. Volkmer, *Cryst. Growth & Des.* **2016**, *16*, 3190-3197; c) S. H. Jhung, J. H. Lee, J. W. Yoon, C. Serre, G. Ferey, J. S. Chang, *Adv. Mater.*

- 2007, 19, 121-124; d) S. Dang, Q. L. Zhu, Q. Xu, *Nat. Rev. Mater.* **2018**, 3, 14.
- [26] a) X. Xiao, L. L. Zou, H. Pang, Q. Xu, *Chem. Soc. Rev.* **2020**, 49, 301-331. b) M. Panchal, F. Nouar, C. Serre, M. Benzaqui, S. Sene, N. Steunou, M.G. Marques, EP 17305119.4, **2017**.
- [27] G. Zahn, P. Zerner, J. Lippke, F. L. Kempf, S. Lilienthal, C. A. Schröder, A. M. Schneider, P. Behrens, *CrystEngComm* **2014**, 16, 9198-9207.
- [28] F. Ragon, P. Horcajada, H. Chevreau, Y. K. Hwang, U. H. Lee, S. R. Miller, T. Devic, J. S. Chang, C. Serre, *Inorg. Chem.* **2014**, 53, 2491-2500.
- [29] F. Ragon, H. Chevreau, T. Devic, C. Serre, P. Horcajada, *Chem. Eur. J.* **2015**, 21, 7135-7143.
- [30] H. Xu, S. Sommer, N. L. N. Broge, J. Gao, B. B. Iversen, *Chem. Eur. J.* **2019**, 25, 2051-2058.
- [31] M. Taddei, N. Casati, D. A. Steitz, K. C. Dümbgen, J. A. van Bokhoven, M. Ranocchiari, *CrystEngComm* **2017**, 19, 3206-3214.
- [32] P. Silva, S. M. F. Vilela, J. P. C. Tome, F. A. A. Paz, *Chem. Soc. Rev.* **2015**, 44, 6774-6803.
- [33] A. U. Czaja, N. Trukhan, U. Muller, *Chem. Soc. Rev.* **2009**, 38, 1284-1293.
- [34] X. Liu, X. Wang, F. Kapteijn, *Chem. Rev.* **2020**, 120, 8303-8377.



Several micro/ mesoporous metal(IV)-based MOFs with different functional groups were synthesized at room temperature using environmentally friendly conditions. The versatility of this strategy allows the use of different reactants and the control of the MOF particle size. A synthesis using a pilot scale-up system demonstrates the potential of this approach for the industrial production of metal (IV)-based MOFs.